2003-11-28

Functional interaction between the Bloom's syndrome helicase and the RAD51 paralog, RAD51L3 (RAD51D).

Braybrooke, JP

http://hdl.handle.net/10026.1/10297

10.1074/jbc.M308838200
J Biol Chem

THE JOURNAL OF BIOLOGICAL CHEMISTRY
Vol. 278, No. 48, Issue of November 28, pp. 48357–48366, 2003
Printed in U.S.A.

Functional Interaction between the Bloom's Syndrome Helicase and the RAD51 Paralog, RAD51L3 (RAD51D)*

Received for publication, August 11, 2003, and in revised form, September 12, 2003
Published, JBC Papers in Press, September 15, 2003, DOI 10.1074/jbc.M308838200

Jeremy P. Braybrooke‡§, Ji-Liang Li‡§, Leonard Wu‡, Fiona Caple¶, Fiona E. Benson¶, and Ian D. Hickson‡‖

From ‡Cancer Research UK, Weatherall Institute of Molecular Medicine, University of Oxford, John Radcliffe Hospital, Oxford OX3 9DS, United Kingdom and the ¶Department of Biological Sciences, Lancaster Environment Centre, Lancaster University, Lancaster LA1 4YQ, United Kingdom

Bloom's syndrome (BS) is a genetic disorder associated with short stature, fertility defects, and a predisposition to the development of cancer. BS cells are characterized by genomic instability; in particular, a high rate of reciprocal exchanges between sister-chromatids and homologous chromosomes. The BS gene product, BLM, is a helicase belonging to the highly conserved RecQ family. BLM is known to form a complex with the RAD51 recombinase, and to act upon DNA intermediates that form during homologous recombination, including D-loops and Holliday junctions. Here, we show that BLM also makes a direct physical association with the RAD51L3 protein (also known as RAD51D), a so-called RAD51 paralog that shows limited sequence similarity to RAD51 itself. This interaction is mediated through the N-terminal domain of BLM. To analyze functional interactions between BLM and RAD51L3, we have purified a heteromeric complex comprising RAD51L3 and a second RAD51 paralog, XRCC2. We show that the RAD51L3-XRCC2 complex stimulates BLM to disrupt synthetic 4-way junctions that model the Holliday junction. We also show that a truncated form of BLM, which retains helicase activity but is unable to bind RAD51L3, is not stimulated by the RAD51L3-XRCC2 complex. Our data indicate that the activity of BLM is modulated through an interaction with the RAD51L3-XRCC2 complex, and that this stimulatory effect on BLM is dependent upon a direct physical association between the BLM and RAD51L3 proteins. We propose that BLM co-operates with RAD51 paralogs during the late stages of homologous recombination processes that serve to restore productive DNA replication at sites of damaged or stalled replication forks.

Bloom's syndrome (BS)[1] is a rare, autosomal recessive disorder characterized by proportional dwarfism, immunodeficiency, subfertility, and a greatly increased incidence of a wide range of cancers (1, 2). Cell lines derived from individuals with BS display a number of abnormalities, including poor growth and plating, and a strikingly high level of chromosomal instability (3, 4). The characteristic feature of BS cells, which is used in diagnosis of the disorder, is an elevated frequency of genetic recombination events, particularly sister-chromatid exchanges (SCEs) (5). However, this hyper-recombination is not limited to exchanges between sister-chromatids, because interchromosomal homologous recombination also occurs at an elevated rate in BS cells (1, 2)

The gene mutated in BS, which is designated *BLM*, is located on chromosome 15q26.1, and encodes a protein comprising 1417 amino acids with a predicted M_r of 159,000 (6). BLM belongs to the highly conserved RecQ family of DNA helicases (3, 4). Because members of the RecQ family have been identified in all organisms, it seems likely that they perform an important and conserved cellular function. There is a single family member in bacterial and yeast species, but at least five in human cells. Of the five human RecQ-related proteins, defects in three are associated with established genetic disorders. In addition to inactivation of BLM in BS, defects in WRN cause Werner's syndrome (7), and defects in RECQ4 cause Rothmund-Thomson syndrome (8). Like BS, both of these disorders are associated with a high incidence of cancers, although the primary manifestations of Werner's syndrome and Rothmund-Thomson syndrome are premature aging, and skin and skeletal abnormalities, respectively. Where studied, all RecQ helicases unwind simple, partial-duplex DNA molecules in a 3′-5′ direction but are notable for their atypical profile of preferred DNA substrates (9). For example, RecQ helicases, including BLM, are apparently unique among helicases in their ability to efficiently disrupt "alternative" (non-Watson-Crick) DNA structures, including G-quadruplexes, that can form in guanine-rich sequences such as telomeric repeat DNA (9–13). Moreover, RecQ helicases selectively bind to at least two DNA structures that arise during the process of homologous recombination. BLM can disrupt synthetic oligonucleotides that mimic the DNA displacement loop (D-loop) structure generated by DNA strand invasion of single-stranded DNA (ssDNA) into an homologous duplex (14). BLM, WRN, and RecQ also unwind synthetic 4-way junctions (X-junctions) that model the Holliday junction recombination intermediate (9, 15, 16), and BLM and WRN have been shown to catalyze efficient and extensive branch migration of RecA-generated Holliday junctions (15, 17).

The process of homologous recombination in eukaryotic cells requires several proteins, of which the central player is RAD51, the eukaryotic ortholog of *Escherichia coli* RecA (18, 19). RAD51 forms helical filaments on DNA and catalyzes DNA strand invasion and exchange. It is assisted in these processes by the actions of several proteins, including RAD52, RAD54, and replication protein A. In *Saccharomyces cerevisiae*, a het-

* This work was supported by Cancer Research UK (to I. D. H.) and the North West Cancer Research Fund (to F. E. B.). The costs of publication of this article were defrayed in part by the payment of page charges. This article must therefore be hereby marked "*advertisement*" in accordance with 18 U.S.C. Section 1734 solely to indicate this fact.

§ Both authors contributed equally to the results of this work.
‖ To whom correspondence should be addressed. Tel.: 44-1865-222417; Fax: 44-1865-222431; E-mail: ian.hickson@cancer.org.uk.

[1] The abbreviations used are: BS, Bloom's syndrome; SCE, sister-chromatid exchanges; ORF, open reading frame; DTT, dithiothreitol; GST, glutathione *S*-transferase; PBSA, phosphate-buffered saline; BSA, bovine serum albumin; DSB, double strand break.

erodimer of the Rad55 and Rad57 proteins acts as a ScRad51 accessory factor, and stimulates ScRad51-mediated DNA strand transfer activity *in vitro* (20, 21). Rad55 and Rad57 are so-called Rad51 paralogs, because they show limited sequence similarity to Rad51, but do not appear to form nucleoprotein filaments or directly catalyze DNA strand invasion/exchange. In human cells, there are five RAD51 paralogs, although it is unclear whether any of these can strictly be considered as the direct counterpart of yeast Rad55 or Rad57. The human RAD51 paralogs are termed RAD51L1 (also known as RAD51B), RAD51L2 (RAD51C), RAD51L3 (RAD51D), XRCC2, and XRCC3 (22–30). The RAD51L2, XRCC2, and XRCC3 proteins are defective in hamster cell mutants (designated irs3, irs1, and irs1SF, respectively) isolated on the basis of hypersensitivity to ionizing radiation (31). These mutants also show hypersensitivity to a variety of other DNA damaging agents, including DNA cross-linking chemicals, as well as extensive genomic instability (23, 32–34). The human RAD51 paralogs form complexes with each other, but not obviously with RAD51 itself. Various complexes have been purified, including RAD51L2-XRCC3, RAD51L3-XRCC2, RAD51L1/L2, and a larger complex containing RAD51L1/L2/L3-XRCC2 (35–39). The biochemical properties of these complexes have not been characterized in detail, and it still remains unclear why five RAD51 paralogs exist in human cells and what their respective functions might be. Apart from an ATPase activity that is stimulated by DNA, little is known about the catalytic activities displayed by the human RAD51 paralogs. One possible role, identified through an analysis of the RAD51L1/L2 complex, is to assist RAD51 in the assembly of a nucleoprotein filament on ssDNA through modulating the action of replication protein A (38). Although there is no conclusive evidence for a direct interaction between human RAD51 and the human RAD51 paralogs, it is clear that the action of RAD51 *in vivo* is influenced by the presence of the paralogs. The most striking manifestation of this is the failure of RAD51 to localize normally to discrete nuclear foci (thought to be sites of ongoing DNA repair) following exposure to ionizing radiation in the irs1, irs1SF, and irs3 cell lines discussed above (40–42).

In addition to their promotion of DNA transactions associated with homologous recombination (such as Holliday junction branch migration), RecQ helicases interact physically with components of the homologous recombination machinery. For example, several RecQ helicases associate with and are stimulated by replication protein A (43–45). It is not clear, however, whether this is relevant to a role for the complex in DNA recombination or replication. More specifically for recombination, there is a conserved interaction between RecQ helicases and RAD51; both between the human BLM and RAD51 proteins, and between the sole RecQ helicase in *S. cerevisiae*, Sgs1p, and the ScRad51 protein (46). This interaction is mediated by the same domain of the RecQ helicase protein (the extreme C-terminal region in each case) (46) despite a lack of obvious sequence similarity between the C-terminal regions of the BLM and Sgs1 proteins.

In view of the numerous biochemical and genetic connections between RecQ helicases and components of the homologous recombination machinery, we have analyzed whether BLM might interact with the human RAD51 paralogs. Here, we show that the N-terminal domain of BLM binds to the RAD51L3 protein. To address whether this interaction has functional effects on the catalytic activity of BLM, we have purified RAD51L3 in complex with its RAD51 paralog partner, XRCC2. We show that the RAD51L3-XRCC2 heteromeric complex can stimulate the ability of BLM to disrupt model Holliday junction structures, and that this stimulatory effect requires that BLM be capable of interacting physically with the RAD51L3-XRCC2 complex. We present a model whereby BLM cooperates with the homologous recombination machinery to process DNA structures that arise at sites of blocked replication forks in human cells.

MATERIALS AND METHODS

Construction of Plasmids—The plasmids pJB1.1, pJB1.2, pJB3.1, and pJB3.2 have been described previously (47). These plasmids, respectively, contain the full-length XRCC2 open reading frame (ORF) cloned into pGEX4T-1 and pET30a, or the full-length RAD51L3 ORF cloned into pET30a and pGEX4T-1. pJB3.21 was generated by cloning the full-length open reading frame for RAD51L3 into pET21a using EcoRI and NotI sites. The 3′ primer contained an in-frame stop codon.

For two-hybrid analyses, previously reported 3′ constructs of the *BLM* cDNA were utilized (48). These encode the C-terminal domain of BLM from residues 966 to 1417. The RAD51L3 and XRCC2 ORFs were cloned directionally (using 5′ EcoRI and 3′ NotI sites) into the pEG202 yeast two-hybrid "bait" plasmid, to generate pEG3.1 and pEG1.1, respectively. The same ORFs were also cloned into the EcoRI site of the 2-hybrid "prey" plasmid, pJG45, to generate pJG3.1 and pJG1.1, respectively. The oligonucleotides used in the PCR amplification of the ORFs can be obtained upon request. All constructs were verified by DNA sequencing.

Yeast Two-hybrid Analysis—Yeast two-hybrid screens were conducted essentially as described by Wu *et al.* (46). Briefly, the *XRCC2* or *RAD51L3* cDNAs were cloned into the plasmid pEG202 (a gift from Dr. R. Brent) to allow expression of XRCC2 or RAD51L3 bait protein as a fusion to LexA under control of the *ADH* promoter. *RAD51L3* or *XRCC2* were also cloned into plasmid pJG45 (a gift from Dr. R. Brent) to create a translational fusion prey under control of the *GAL1* galactose inducible promoter (49). Plasmids were transformed into yeast strain EGY48, containing the reporter plasmid pSH1834, using the lithium acetate method, as published previously (50). Transformants were selected at 30 °C on SD-agar lacking histidine, tryptophan, and uracil.

Colonies were streaked onto YPD agar plates, which were incubated at 30 °C overnight, before colonies were replica plated onto SD-agar containing galactose, raffinose, and 5-bromo-4-chloro-3-indolyl-β-D-galactopyranoside (X-gal), but lacking histidine, tryptophan, uracil, and leucine. Colonies were considered positive if they grew and turned blue, after overnight incubation at 30 °C. Control proteins, including hRAD51, LexMax, and HM12, were used as preys to assess the specificity of the interaction (51). Further two-hybrid experiments were performed, using fragments of BLM (see Fig. 1) as either bait or prey proteins. Quantitative β-galactosidase assays on liquid cultures were performed as described previously (47).

Preparation of Extracts from Human Cell Lines—Whole cell extracts from human cells were prepared by washing cells in PBSA and then boiling in SDS-PAGE protein loading buffer. Nuclear extracts were prepared from exponentially growing HeLa S3 cells in suspension. Approximately 2×10^8 cells were harvested by centrifugation, the pellet was washed in PBSA, and the cells were lysed in 5 ml of buffer (10 mM Tris-HCl, pH 7.5, 1.5 mM $MgCl_2$, 10 mM NaCl, 1% (v/v) Nonidet P-40, 1 mM DTT), supplemented with protease and phosphatase inhibitors (1 mM sodium fluoride, 1 mM β-glycerophosphate, 1 mM sodium orthovanadate, 5 mM sodium pyrophosphate, 1 mM glucose 1-phosphate, 10 nM microcystin, 0.1 mM *para*-nitrophenylphosphate, 1 mM phenylmethylsulfonyl fluoride, and complete protease inhibitor mixture tablets (Roche Diagnostics) according to the manufacturer's instructions) on ice for 45 min. Nuclei were harvested by centrifugation at $5000 \times g$ for 5 min and the remaining supernatant designated as the "cytoplasmic" fraction. The nuclear pellet was re-suspended in 0.3 ml of TKM buffer (50 mM Tris-HCl, pH 7.5, 5 mM $MgCl_2$, 25 mM KCl, 1 mM DTT, supplemented with protease and phosphatase inhibitors as described above), to which 0.6 ml of buffer D (80 mM Tris-HCl, pH 7.5, 2 mM EDTA, 530 mM NaCl, 1 mM DTT, supplemented with protease and phosphatase inhibitors as above) was added, before incubation on ice for 30 min. The nuclear extract was cleared by centrifugation at 14,000 rpm in a microcentrifuge at 4 °C, and used on the day of preparation.

Co-immunoprecipitations—All steps were performed at 4 °C unless indicated otherwise. Nuclear and cytoplasmic extracts were made as described above. IHIC42 (anti-RAD51L3), IHIC48 (anti-XRCC2) (47), or appropriate preimmune sera were added to the extract at a dilution of 1:100, and the mixture was incubated on ice for 1 h. 100 μl of a 50% (w/v) slurry of protein A-Sepharose (in TKM/buffer D; ratio 1:2) was added, and the mixture was rotated end over end for 30 min at 4 °C. The immunoprecipitates were harvested in a microcentrifuge at 14,000 rpm

for 5 s, and the pellet was washed with 1 ml of TKM/buffer D (ratio 1:2). The pellet was washed a further five times in the same buffer, before being boiled in protein loading buffer. Samples were separated by SDS-PAGE, transferred to nitrocellulose membrane, and Western blotted using conventional methods.

GST "Pull-down" Experiments—Purified RAD51L3-GST or XRCC2-GST fusion proteins were bound to glutathione-agarose columns as described previously (46, 47) using a typical bed volume of 0.5 ml. All constructs for expression of GST fusion proteins have been described previously (47, 48), except for N1-RAD51L3-GST, which was generated using PCR to eliminate the first 120 codons of the RAD51L3 cDNA. Briefly, purified recombinant protein or nuclear extracts were loaded onto the column at 4 °C, and the resin was washed with 15 ml of TKM/buffer D. The column matrix was boiled in protein sample loading buffer and the eluted proteins were separated by SDS-PAGE before Western blotting.

Far Western Blotting Analysis—Typically, 0.2–0.5 μg of each polypeptide was subjected to SDS-PAGE and transferred to Hybond C-extra nitrocellulose membranes using a TE 70 semi-dry transfer unit (Hoeffer). All subsequent steps were performed at 4 °C. Filters were immersed twice in denaturation buffer (6 M guanidine HCl in PBSA) for 10 min, and then incubated for 6 × 10 min in serial dilutions (1:1) of denaturation buffer with PBSA supplemented with 1 mM DTT. Filters were blocked in PBSA containing 10% (w/v) powdered low fat milk, 0.1% (v/v) Tween 20 for 30 min before being incubated with purified recombinant RAD51L3 protein (47) in PBSA supplemented with 0.25% (w/v) milk, 0.1% (v/v) Tween 20, 1 mM DTT, and 1 mM phenylmethylsulfonyl fluoride for 60 min. Filters were washed for 4 × 10 min in PBSA containing 0.25% (w/v) powdered low fat milk, 0.1% (v/v) Tween 20. The second wash contained 0.00001% (v/v) glutaraldehyde. Conventional Western analysis was then performed to detect the presence of RAD51L3 using IHIC42 as the primary antibody. An otherwise identically treated negative control blot was processed, but without any incubation with RAD51L3.

Purification of the RAD51L3-XRCC2 Complex—BL21(DE3) bacteria were transformed simultaneously with pJB3.21 and pJB1.2, and transformants were selected on LB agar containing ampicillin and kanamycin. Cultures of the doubly transformed bacteria were grown in LB medium containing ampicillin and kanamycin at 37 °C to an A_{600} of 0.6 before addition of isopropyl-1-thio-β-D-galactopyranoside to a final concentration of 0.4 mM. After 2 h of incubation with shaking, the culture was cooled to 4 °C in iced water for 15 min, and the cells were harvested by centrifugation. The cell pellet was re-suspended in 25 mM Tris-HCl, pH 7.5, 250 mM NaCl (1 ml of buffer per 40 ml of original bacterial culture volume), and the suspension was frozen at −80 °C. Following thawing of the suspension, all procedures were carried out at 4 °C unless stated otherwise. 0.2% (v/v) Triton X-100 and complete EDTA-free protease inhibitor tablets (Roche Diagnostics) were added and the mixture was incubated on ice for 30 min. Phenylmethylsulfonyl fluoride was added to the final concentration of 1 mM immediately prior to lysis by sonication (4 × 15 s at maximum amplitude with cooling on ice between bursts). The lysate was cleared by centrifugation at 39,000 rpm for 25 min (70 Ti rotor; Beckman) and ammonium sulfate was added to a final concentration of 45% to precipitate proteins. Following incubation on ice for 30 min, precipitated proteins were harvested by centrifugation, the pellet was re-suspended in 25 mM Tris-HCl, pH 7.5, 100 mM NaCl, and the solution was dialyzed for 2 h against nickel binding buffer (25 mM Tris-HCl, pH 7.5, 450 mM NaCl, 10 mM imidazole). The solution was then subjected to nickel chelate chromatography using a Poros MC20 column with a bed volume of 1.7 ml and a BioCAD work station (Perceptive Biosytems). Prior to loading, the column was charged with several bed volumes of 100 mM $NiSO_4$, saturated with 5 bed volumes of 1.5 M imidazole in 25 mM Tris-HCl, pH 7.5, 450 mM NaCl, and finally was equilibrated with 5 bed volumes of 10 mM imidazole in the same buffer. After loading of the protein sample, the column was washed with 25 bed volumes of the loading buffer containing 100 mM imidazole. Elution was performed with an imidazole gradient of 100–500 mM in the same buffer, applied over 8 bed volumes. 1-ml fractions were collected and those containing recombinant protein, as determined by spectrophotometric monitoring (A_{280}) and SDS-PAGE, were dialyzed at 4 °C for 4 h against heparin binding buffer containing 25 mM Tris-HCl, pH 7.5, 50 mM NaCl, 1 mM EDTA, 1 mM DTT. The dialyzed solution was loaded onto a heparin-agarose column (Pierce) at 4 °C, the column was washed with 10 bed volumes of loading buffer containing 100 mM NaCl, and bound proteins were eluted in the same buffer containing 600 mM NaCl. Fractions containing recombinant RAD51 paralog proteins were identified by SDS-PAGE. These fractions were dialyzed into buffer containing 25 mM Tris-HCl, pH 7.5, 50 mM NaCl, 1 mM EDTA, 1 mM DTT, 10% (v/v) glycerol. The dialyzed solution was loaded onto a 1-ml FPLC Mono Q (Amersham Biosciences), the column was washed with loading buffer containing 100 mM NaCl, and bound proteins were eluted with a NaCl gradient from 100 to 600 mM. The fractions were analyzed by SDS-PAGE, and those containing the purified RAD51L3-XRCC2 complex were dialyzed overnight against buffer containing the 25 mM Tris-HCl, pH 7.5, 50 mM NaCl, 1 mM EDTA, 1 mM DTT, 10% glycerol. Protein samples were stored in aliquots at −80 °C. Confirmation that the purified proteins were RAD51L3 and XRCC2 was provided by Western blotting analyses of the purified fractions using mouse monoclonal antibodies to the hexahistidine tag (anti-polyhistidine; Sigma, H-1029) or the T7 tag (Novagen). Further confirmation was provided by Western blotting with rabbit polyclonal antibodies to RAD51L3 (IHIC42), and to XRCC2 (IHIC48), which have been described previously (47). Protein concentration was determined using a colorimetric assay (Bio-Rad protein assay), according to the manufacturer's instructions.

Preparation of Radiolabeled Oligonucleotides—200 ng of oligonucleotide was incubated with 5–10 units of T4 polynucleotide kinase (New England Biolabs), 25 μCi of [γ-^{32}P]ATP (3000 Ci/mmol) in the manufacturer's buffer, in a total volume of 10 μl, for 30 min at room temperature. The reaction was stopped by the addition of 50 μl of STE buffer (20 mM Tris-HCl, pH 7.5, 100 mM NaCl, 10 mM EDTA) before separation of the oligonucleotide from the unincorporated ATP using a "Mini Quick spin DNA column" (Roche Diagnostics) according to the manufacturer's instructions.

The synthetic 4-way junction (X-junction) was created by annealing the four oligonucleotides described previously (15), and purified by electrophoresis on a 10% non-denaturing polyacrylamide gel. The substrates were stored at −20 °C until required.

ATPase Assays—ATPase activity was determined by the release of [γ-^{32}P]P_i from [γ-^{32}P]ATP. The assay mixture (20 μl) contained 25 mM Tris-HCl, pH 7.5, 1 mM EDTA, 1 mM DTT, 100 μg/ml BSA, 100 mM NaCl, 2.5 mM $MgCl_2$ (or other divalent metal ion), 25 μg/ml DNA (76 μM nucleotides), 200 μM ATP, 50 nCi of [γ-^{32}P]ATP (3000 Ci/mmol), and 1.0 μM recombinant protein. After incubation at 37 °C for up to 2 h, the reaction was stopped by the addition of 10 μl of 0.5 M EDTA. 1 μl of each reaction was spotted onto CEL 300 PEI/UV_{254} (Polygram) thin layer chromatography plates, which were rinsed in 100% methanol before separation of [γ-^{32}P]P_i from [γ-^{32}P]ATP in buffer containing 0.8 M LiCl, 0.8 M acetic acid. Plates were exposed on PhosphorImager screens (Amersham Biosciences) and the percentage release of [γ-^{32}P]P_i quantified using ImageQuant software (Amersham Biosciences). K_{cat} calculations were carried out using the initial linear portion of plots of P_i release *versus* reaction time.

DNA Binding Assays—5′ end-labeled ^{32}P single-stranded or double-stranded oligonucleotides were prepared as described previously. Typically, 1 nmol of each oligonucleotide was incubated with protein in 25 mM Tris-HCl, pH 7.5, 0.1 mg/ml BSA, 1 mM DTT, and 1 mM EDTA with or without 2 mM ATP and 2.5 mM $MgCl_2$ at room temperature for 15 min. Protein-DNA complexes were separated on 5% non-denaturing TBE polyacrylamide gels at 4 °C, dried onto 3MM (Whatman) filter paper, and visualized by autoradiography.

DNA Helicase Assays—The synthetic 4-way junction (X-junction) DNA was prepared as described previously (15). Reactions (20 μl final volume) were carried out in buffer containing 50 mM Tris-HCl, pH 7.5, 2 mM $MgCl_2$, 2 mM ATP, 0.1 mM DTT, 100 μg/ml BSA, and 0.5 mg/ml yeast tRNA. BLM (concentration 0.5–1.5 nM) and RAD51L3-XRCC2 (concentration 1–50 nM) were pre-mixed on ice, before addition of the 5′ ^{32}P-end-labeled X-junction substrate. Reactions were incubated at 37 °C for 20–45 min before being stopped and de-proteinized by the addition of a one-fifth volume of stop buffer (5× is 100 mM Tris-HCl, pH 7.5, 100 mM $MgCl_2$, 3% (v/v) SDS, and 10 mg/ml proteinase K). After a further incubation at 37 °C for 30 min, samples were separated by electrophoresis through 10% non-denaturing TBE polyacrylamide gels. Gels were dried on 3MM (Whatman) filter paper before being visualized on PhosphorImager screens. % DNA unwinding was quantified using ImageQuant software (Amersham Biosciences).

RESULTS

RAD51L3 Interacts with the N-terminal Domain of BLM—To analyze whether RAD51L3 and/or XRCC2 can interact with the BLM helicase, yeast two-hybrid analyses were performed using the system developed by Zervos *et al.* (51), as described previously (46). The full-length RAD51L3 and XRCC2 cDNAs were cloned in-frame into both pEG202 and pJG45 (see "Materials and Methods"). Various fragments of the N-terminal and C-

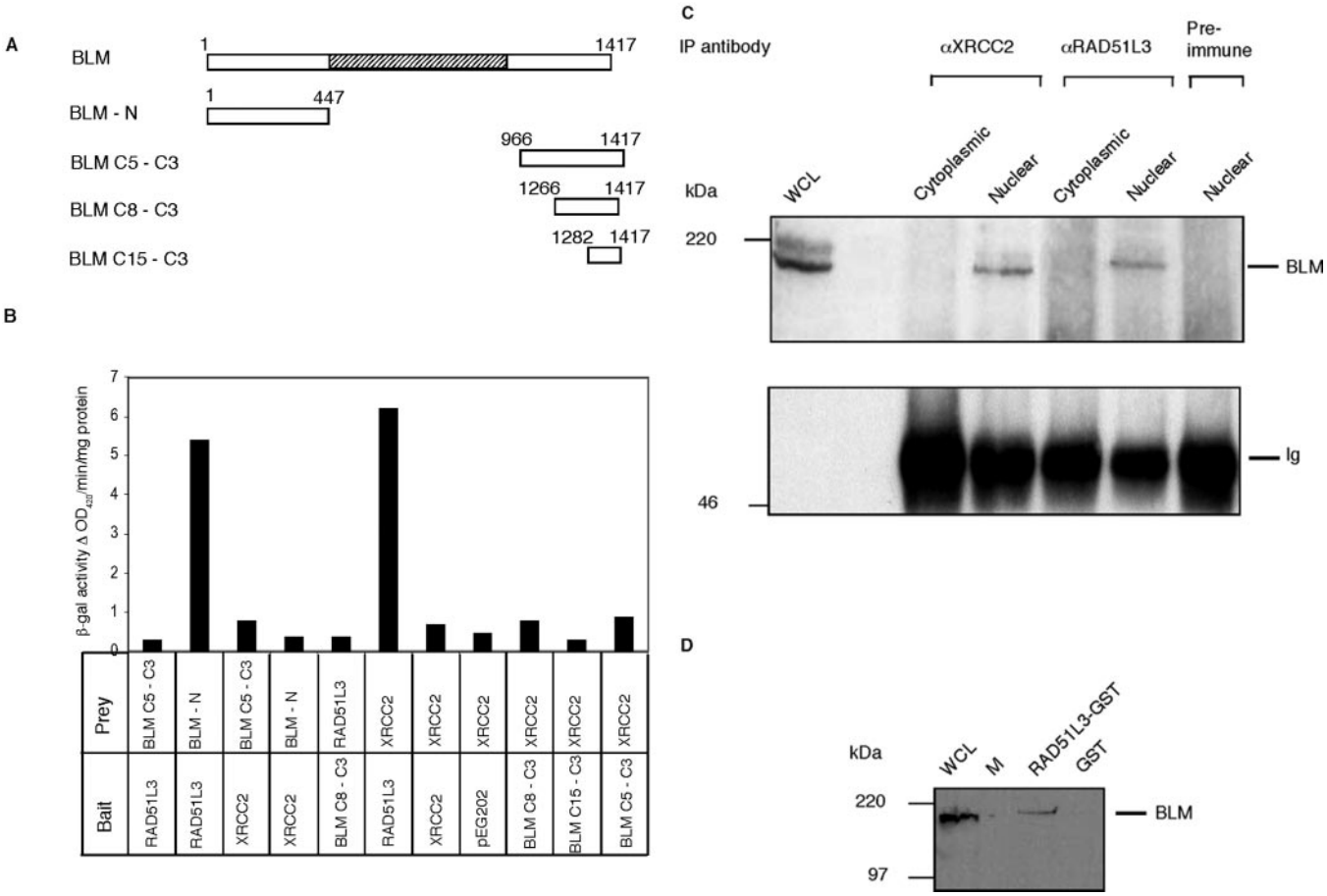

FIG. 1. **BLM interacts with RAD51L3.** *A*, schematic representation of the fragments of the BLM protein used in yeast two-hybrid analyses. The full-length BLM (*top*) comprises 1417 amino acids, including a central helicase domain (*cross-hatched*). *Numbers* refer to residue numbers in BLM. *B*, yeast two-hybrid analysis of different bait proteins (expressed from pEG202) and prey proteins (expressed from pJG45). Data are the level of β-galactosidase (β-gal) activity for each combination of bait and prey. XRCC2 and RAD51L3 were included as a positive control. Values represent the mean of two independent experiments. *C*, co-immunoprecipitation of BLM with antibodies to RAD51L3 or XRCC2. Nuclear or cytoplasmic extracts from HeLa cells were incubated with IHIC48 (anti-XRCC2), IHIC42 (anti-RAD51L3), or preimmune serum. Bound proteins were precipitated with Protein A-Sepharose. Following extensive washing, precipitated proteins were separated by SDS-PAGE and transferred to nitrocellulose. Filters were Western blotted with IHIC33 (anti-BLM). The positions of BLM and the immunoglobulin heavy chain marker of loading (Ig) are indicated. *WCL* indicates a whole cell lysate that was run on the gel in parallel to denote the mobility of full-length BLM. *D*, pull-down of BLM from a HeLa cell nuclear extract by a RAD51L3-GST fusion protein but not by GST alone. The position of BLM is indicated. *Lanes WCL* and *M* represents a whole cell lysate and molecular mass standards, respectively.

terminal domains of BLM were also cloned into these vectors, as described previously (46). Fig. 1*A* shows schematically the various BLM fragments analyzed. When present in the pEG202 bait plasmid, the N-terminal domain of BLM autoactivated gene expression when expressed in EGY48 yeast cells, even in the absence of a prey plasmid, and therefore this construct was not studied further. This autoactivation probably results from the presence of blocks of acid residues in the N-terminal domain of BLM that can serve as transcriptional activation domains. Hence, the N-terminal domain of BLM was analyzed only in the prey plasmid. A positive interaction in the yeast two-hybrid system (as indicated by the blue coloration of yeast colonies) was found between the N-terminal domain of BLM (BLM-N) and RAD51L3, but not between the C-terminal domain of BLM and RAD51L3. The extent of interaction between the N-terminal domain of BLM and RAD51L3 was quantified be measuring β-galactosidase activity in yeast cultures. A comparable level of β-galactosidase activity was seen in yeast containing BLM-N and RAD51L3 as was seen with the positive control (RAD51L3 and XRCC2) (Fig. 1*B*). As expected from the lack of blue coloration in yeast colonies, the quantitative assay revealed background β-galactosidase activity in cultures containing BLM-C and RAD51L3, and those containing XRCC2 and either BLM-N or BLM-C (Fig. 1*B*). Despite the fact that no interaction was found between XRCC2 and any of the BLM fragments analyzed, the possibility remains that XRCC2 interacts with the central helicase domain of BLM that was not included in this study.

To determine whether BLM interacts with RAD51L3 *in vivo*, immunoprecipitation experiments were performed. For this, both nuclear and cytoplasmic fractions of HeLa cell extracts were prepared, and immunoprecipitation of RAD51L3 (using the IHIC42 antibody) or XRCC2 (using the IHIC48 antibody) was carried out as described under "Materials and Methods." Preimmune sera were used as controls. BLM could be co-immunoprecipitated with both anti-RAD51L3 and anti-XRCC2 antibodies, but not with the preimmune serum controls (Fig. 1*C*). Moreover, this co-imunoprecipitation occurred only when a nuclear protein extract was analyzed, consistent with the known localization of BLM and the RAD51 paralogs to the nucleus in human cells. Although the reciprocal immunoprecipitations were attempted (*i.e.* precipitation with anti-BLM antibodies and Western blotting for RAD51L3 or XRCC2) inconclusive results were obtained, primarily because the intense signal representing the immunoglobulin heavy chain masked the region of the membrane where RAD51L3 and XRCC2 would be expected to be found (data not shown). As an alternative approach to confirming the interaction, pull-down ex-

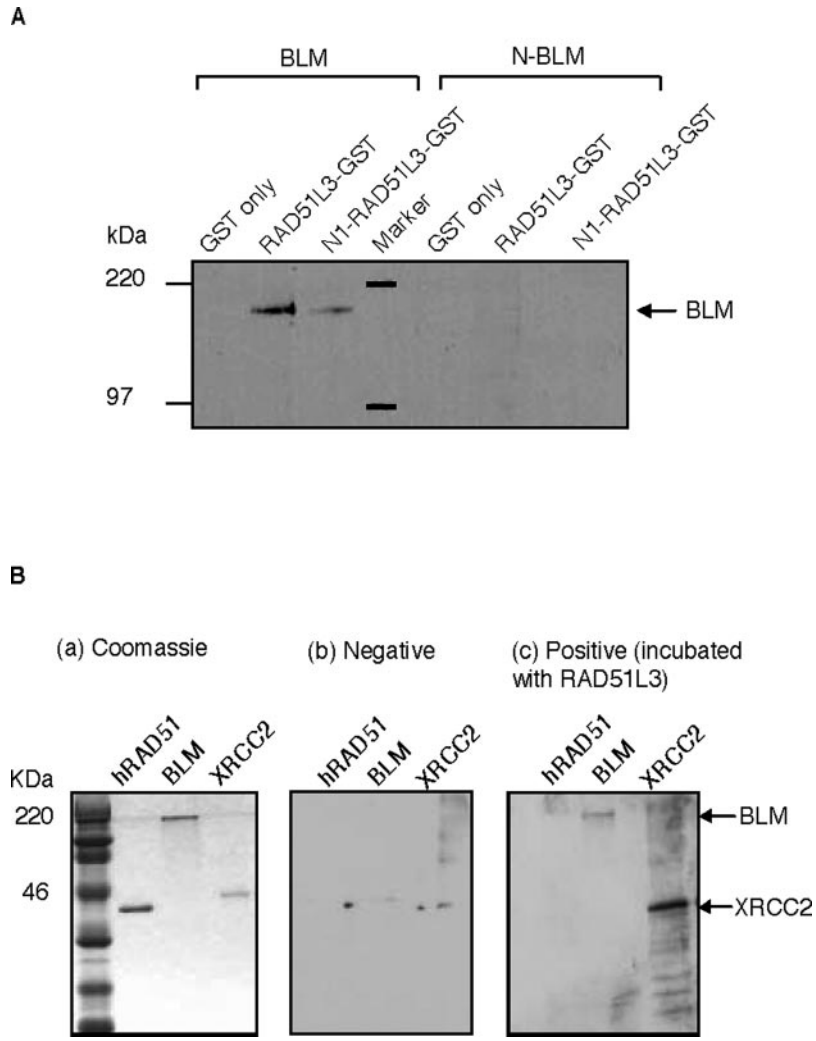

FIG. 2. **BLM interacts directly with RAD51L3**. *A*, RAD51L3 can pull-down purified full-length BLM but not N-terminal truncated BLM. RAD51L3-GST (full-length) or an N-terminal truncated RAD51L3 (N1-RAD51L3) were bound to glutathione-agarose beads and incubated with BLM or N-BLM. After extensive washing of the beads, bound proteins were separated by SDS-PAGE and Western blotted with IHIC33 anti-BLM antibodies. The position of BLM is indicated by the *arrow*. The positions where the 220- and 97-kDa molecular mass standards migrated is indicated in the maker lane by *black horizontal bars*. ***B***, far Western blotting analysis. BLM, hRAD51, and XRCC2 were separated by SDS-PAGE and proteins stained with Coomassie Blue (*panel a*). Two identical membranes were prepared for Western blotting. The negative membrane (*panel b*) was incubated with buffer alone, whereas the positive membrane was incubated with purified RAD51L3. The membranes were then probed using IHIC42 (anti-RAD51L3). Note the positive signals in *panel c* in the positions where BLM and XRCC2 are located, but not where hRAD51 is located.

periments were performed on HeLa cell nuclear extracts using a RAD51L3-GST fusion protein, or GST protein alone as a control. Fig. 1*D* shows that the RAD51L3-GST fusion protein readily pulled down BLM from the extract, whereas the control GST fusion protein could not, confirming the specificity of the interaction.

Next, we analyzed whether the interaction between RAD51L3 and BLM is a direct one, because the data presented thus far could indicate that the interaction is mediated through an adapter protein or DNA. For this section of the study, two approaches were undertaken. First, GST pull-down experiments were performed using purified proteins. Fig. 2*A* shows that full-length recombinant BLM could be pulled down both with RAD51L3-GST and with a truncated RAD51L3-GST fusion protein, designated N1-RAD51L3-GST, which lacks the first 120 amino acids of RAD51L3. Consistent with the yeast two-hybrid data presented above indicating that the RAD51L3 interaction domain resides in the N-terminal domain of BLM, RAD51L3-GST did not pull-down a truncated version of BLM (N-BLM) lacking residues 1–212 of the BLM protein. Taken together, these results indicate that RAD51L3 interacts directly with BLM and that the first 212 amino acids of BLM are important for this interaction. In contrast, the first 120 amino acids of RAD51L3 are apparently not required for mediating the interaction with BLM.

In a second approach to confirming that RAD51L3 and BLM interact directly, far Western blotting analysis was performed (Fig. 2*B*). Three purified proteins, RAD51, BLM, and XRCC2, were run on a standard SDS-polyacrylamide gel (*panel a*) and then transferred to a nitrocellulose membrane. RAD51 and XRCC2 were included to act as negative and positive controls, respectively, for revealing any interaction between BLM and RAD51L3. Two identical membranes were generated, one of which, the "negative" blot (*panel b*), was incubated with buffer alone. The "positive" blot (*panel c*) was incubated with purified RAD51L3, as described under "Materials and Methods." Both membranes were then probed with IHIC42 to detect any RAD51L3 bound to any of the three proteins present on the membrane. A positive signal was seen at the positions where BLM and XRCC2 were located, but no specific signal was seen in the lane containing RAD51, or on the negative blot. It should be noted that the XRCC2-specific signal was consistently stronger than the BLM-specific signal on these blots, which may reflect differences in the relative affinity of interaction between each of these proteins and RAD51L3. These results confirm that RAD51L3 interacts directly with both BLM and XRCC2, and are consistent with previous data (39) suggesting a lack of a direct interaction between RAD51L3 and RAD51.

Purification of a Heteromeric Complex of RAD51L3 and XRCC2—Several previous analyses have indicated that the successful purification of individual human RAD51 paralogs as recombinant proteins is problematical. We have reported previously the isolation of RAD51L3 in limited quantities (47), but our attempts to purify XRCC2 from *E. coli* proved unsuccessful, because of an inability to express the protein in a soluble form (data not shown). We reasoned that co-expression of RAD51L3

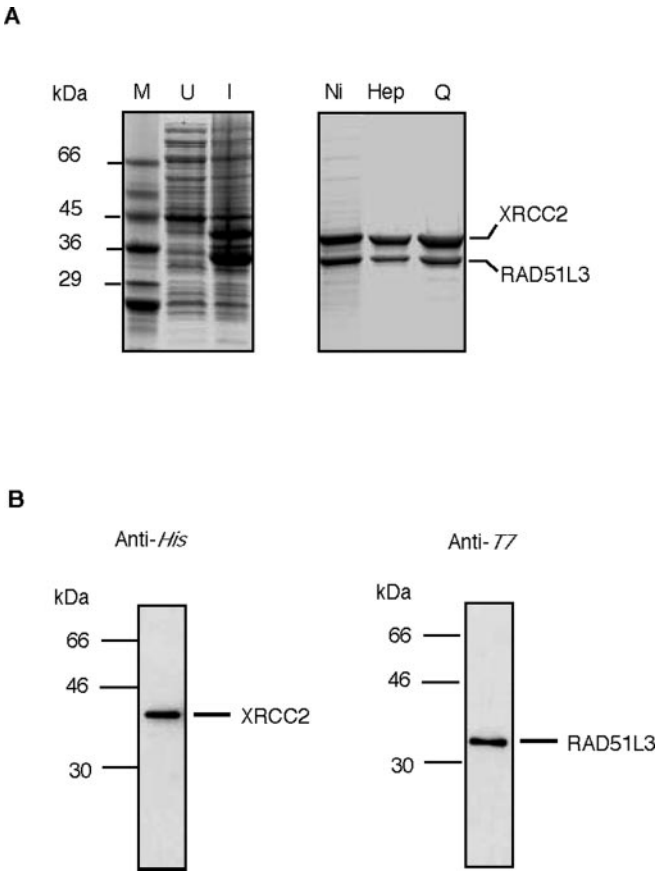

FIG. 3. **Co-expression and purification of a heteromeric complex of RAD51L3 and XRCC2.** *A*, the RAD51L3 and XRCC2 proteins were co-expressed in *E. coli* as described under "Materials and Methods." Protein extracts were prepared from uninduced (*U*) or induced (*I*) bacterial cultures (*left panel*), and the complex was purified by nickel chelate chromatography (*Ni*), heparin affinity chromatography (*Hep*), and FPLC Mono Q chromatography (*Q*) (*right panel*). The positions of the XRCC2 and RAD51L3 proteins are indicated on the *right*. *M* denotes molecular mass standards. *B*, Western blot using anti-His tag antibodies (for XRCC2; *left panel*) and anti-T7 tag antibodies for RAD51L3 (*right panel*) of the purified RAD51L3-XRCC2 complex.

and its partner XRCC2 may help in the solubilization of these proteins, and therefore would permit purification of milligram quantities of the complex. To this end, we subcloned the *RAD51L3* and *XRCC2* cDNAs into the pET21a and pET30a expression vectors, to generate pJB3.21 and pJB1.1, respectively (see "Materials and Methods"). pJB3.21 directs expression of RAD51L3 including an N-terminal T7 epitope tag, whereas pJB1.2 directs expression of an N-terminal hexahistidine-tagged XRCC2 protein. The two constructs were co-transformed into *E. coli* BL21(DE3) cells and the proteins were induced by treatment of the culture with isopropyl-1-thio-β-D-galactopyranoside (see "Materials and Methods"). The complex of RAD51L3-XRCC2 proteins was then purified by ammonium sulfate precipitation, followed by chromatography on nickel chelate resin, and heparin-Sepharose and FPLC Mono Q columns. The RAD51L3 and XRCC2 protein co-purified through all of these purification steps and the RAD51L3-XRCC2 complex was judged to be greater than 95% pure following Mono Q chromatography (Fig. 3*A*). Based on Coomassie Blue staining, it would appear that the RAD51L3 and XRCC2 proteins are present in approximately equal proportions in the purified complex. Western blotting with anti-His tag antibodies (for XRCC2) or anti-T7 tag antibodies (for RAD51L3) (Fig. 3*B*) indicated that the two purified proteins did indeed represent RAD51L3 and XRCC2. This was confirmed using the IHIC42 and IHIC48 antibodies specific for RAD51L3 and XRCC2, respectively (47). A similar scheme for co-expression of the RAD51L3-XRCC2 complex has been reported recently by others (35).

Biochemical Properties of the RAD51L3-XRCC2 Complex—In addition to utilizing the purified RAD51L3-XRCC2 complex for an analysis of possible interactions with BLM, we also investigated some of the possible biochemical properties of the complex itself. It is well established that RAD51 is a weak ATPase. We have shown previously that RAD51L3 is also a weak ATPase, with maximal stimulation being observed when ssDNA is used as a co-factor (47). We found that the purified RAD51L3-XRCC2 complex possessed an ATPase activity that was substantially stimulated by ssDNA, but less strongly stimulated by double strand DNA (Fig. 4). The ATPase activity of the complex required Mg^{2+} ions, although Mn^{2+} (but not Zn^{2+} or Co^{2+}) ions could substitute to some extent (~10% of the rate in the presence of Mg^{2+}). The optimal Mg^{2+} ion concentration was 1–2 mM (data not shown). The turnover number (K_{cat}) for the ATPase activity of RAD51L3-XRCC2 in the presence of ssDNA was determined to be 0.34 molecules of ATP hydrolyzed/min/protein monomer, marginally above that for RAD51L3 alone (0.26) or for RAD51 protein (0.17). There was no indication of a synergistic stimulation of ATPase activity when RAD51 and the RAD51-XRCC2 complex were mixed in various ratios (data not shown). In common with RAD51L3, the RAD51L3-XRCC2 complex was shown using gel retardation assays to bind to ssDNA, but less efficiently to double strand DNA (data not shown). Additional biochemical analyses performed on the RAD51L3-XRCC2 complex are reviewed under "Discussion."

The RAD51L3-XRCC2 Complex Interacts Functionally with the BLM Helicase—Because of the connections between BLM, the RAD51L3-XRCC2 complex, and homologous recombination reactions, we next analyzed whether BLM might interact functionally with this RAD51 paralog complex. To this end, we studied the efficiency with which BLM can disrupt a synthetic 4-way junction (X-junction) that is a model for the Holliday junction recombination intermediate in the presence and absence of the RAD51L3-XRCC2 complex. The data in Fig. 5, *A* and *B*, show that the rate of BLM-mediated disruption of the synthetic Holliday junction was increased ~3-fold in reactions containing the RAD51L3-XRCC2 complex. Incubation of the substrate with the paralog complex alone gave no detectable junction unwinding, indicating that the stimulation of BLM was not because of the presence of a contaminating helicase/branch migration protein in the paralog complex preparation. One trivial explanation for the stimulation of BLM by RAD51L3-XRCC2 is that the paralog complex binds to the ssDNA-containing products of the BLM reaction, and that by doing so relieves product inhibition of the reaction and/or prevents renaturation of the substrate. This possibility can be eliminated, however, because it is known that the *E. coli* single strand-binding protein, an avid ssDNA binding factor, does not stimulate BLM activity (44).

As discussed above, residues 1–212 of BLM appear to be vital in mediating the interaction with RAD51L3. We have reported previously the purification of a truncated form of BLM (termed BLM-NC) that lacks residues 1–212, as well as the final 150 amino acids at the C-terminal end of the protein (52). The BLM-NC protein is catalytically active, and has been shown to unwind the same broad range of DNA substrates as reported for the full-length BLM protein, including 3′-tailed partial duplexes and G-quadruple DNA (52). In the current study, we showed that the BLM-NC protein was also able to disrupt a synthetic X-junction in a time- and concentration-dependent

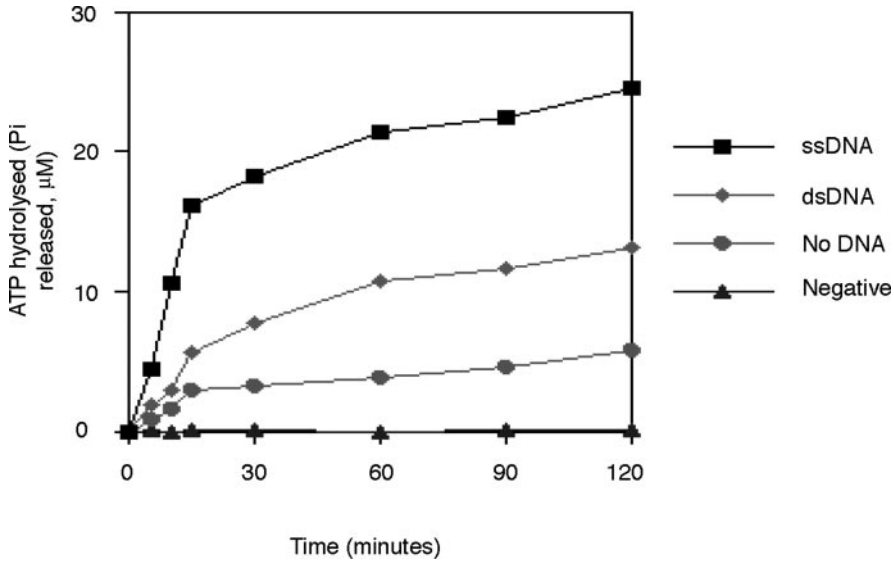

FIG. 4. **The RAD51L3-XRCC2 complex is a DNA-stimulated ATPase**. Time course of ATP hydrolysis catalyzed by the RAD51L3-XRCC2 complex in the presence or absence of ssDNA or double strand DNA co-factor. Heat-denatured protein was used as the negative control.

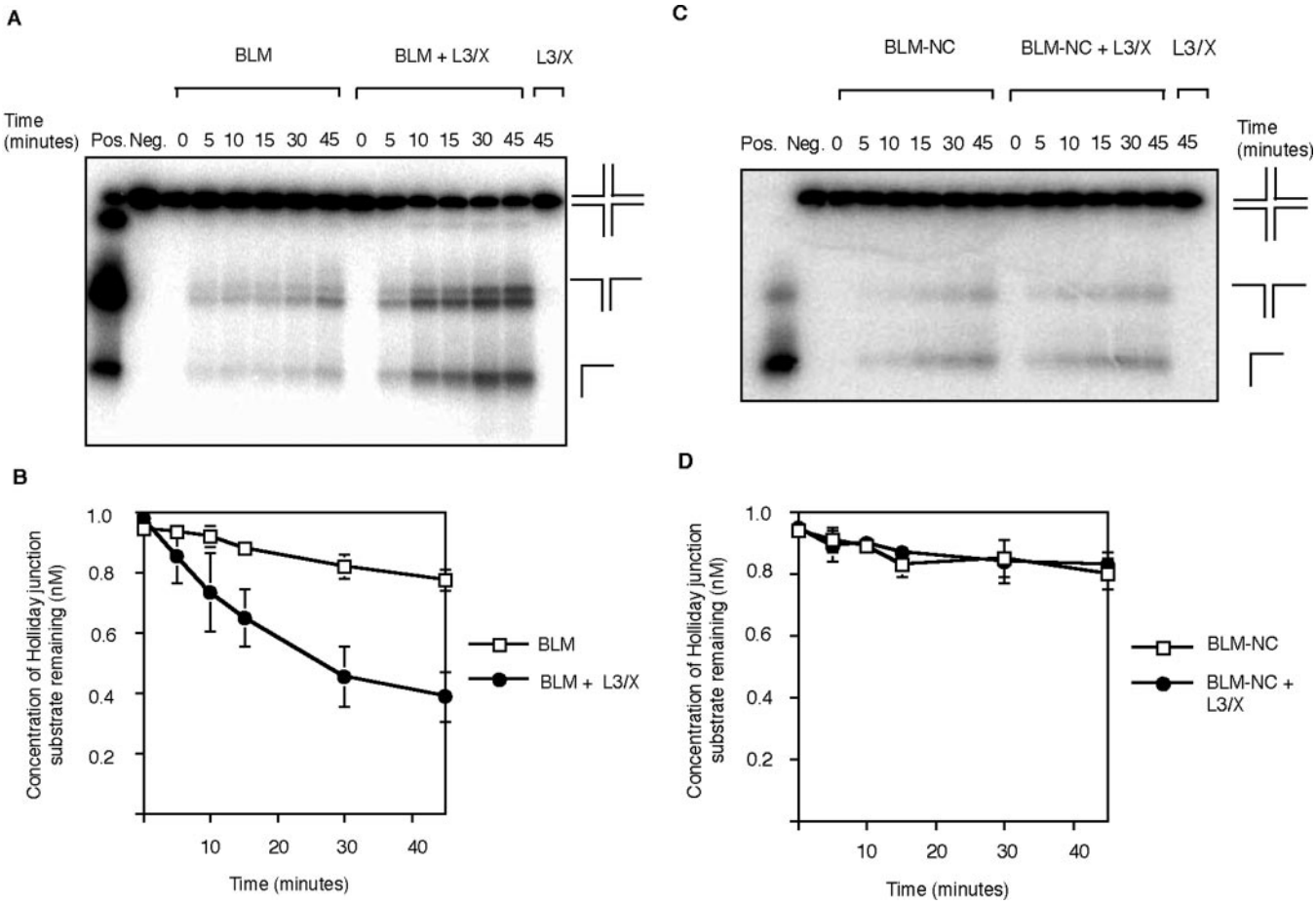

FIG. 5. **The RAD51L3-XRCC2 complex stimulates BLM to disrupt a synthetic 4-way junction.** *A*, autoradiograph of an X-junction disruption assay. A time course of reactions containing 4 nM BLM alone or 4 nM BLM plus 20 nM RAD51L3-XRCC2 (*L3/X*) complex (as indicated *above* the lanes). The positions of the 4-way junction substrate, the two forms of 2-way junctions products, and the fully unwound ssDNA product are indicated diagrammatically on the *right*. Control lanes: *Pos*, *Neg* (both far left), and *L3/X* (far right) represent boiled substrate, no protein control, and a reaction lacking BLM but containing RAD51L3-XRCC2, respectively. *B*, quantification of the data from *panel A*. *C*, identical 4-way junction disruption assays to those shown in *panel A*, except BLM was replaced by the truncated BLM-NC protein. *D*, quantification of the data from *panel C*.

manner (Fig. 5, *C* and *D*, and data not shown). In contrast to the results presented in Fig. 5*A*, we were unable to demonstrate any modulation of BLM-NC-mediated X-junction unwinding activity by the RAD51L3-XRCC2 complex. These data indicate that the stimulation of the activity of full-length BLM by the paralog complex requires that the BLM and RAD51L3 proteins be able to interact physically. These results also confirm that the observed stimulation of full-length BLM is not a nonspecific effect either of ssDNA binding by the paralog complex, or of overall protein concentration in reactions containing the RAD51L3-XRCC2 complex. Consistent with this, we also did not observe stimulation of BLM by the addition to unwind-

ing reactions of other "nonspecific" proteins, such as BSA or GST (data not shown).

DISCUSSION

We have shown that the BS gene product, BLM, interacts physically and directly with the RAD51L3 protein. This interaction is mediated by the N-terminal domain of BLM. We have purified RAD51L3 in a complex with its RAD51 partner paralog, XRCC2, and shown that this complex can stimulate the ability of BLM to disrupt a synthetic Holliday junction substrate.

We have presented several lines of independent evidence that BLM interacts with RAD51L3. This interaction is direct, as evidenced by the finding that the two purified proteins can form a complex *in vitro*. Similarly, BLM interacts directly with RAD51 itself (46). Although we were able to co-immunoprecipitate BLM and XRCC2 from HeLa cell nuclear extracts, we obtained no evidence for a direct interaction between these two proteins. The most likely explanation for this co-immunoprecipitation is that the association is mediated by RAD51L3 serving as a protein bridge between BLM and XRCC2. Consistent with this interpretation is the now established tight association between RAD51L3 and XRCC2, and the indication that, although multiple combinations of human RAD51 paralog complexes have been isolated, XRCC2 appears to only associate directly with RAD51L3 (35–38, 47). The dramatic improvement in solubility of the recombinant RAD51 paralogs when co-expressed in *E. coli* (35) is strong evidence for the functional importance of complex formation between these different paralogs, and suggests that RAD51L3 and XRCC2 are unlikely to exist as isolated proteins *in vivo*. This interpretation is consistent with results from previous studies (35–38,47).

We have shown that the RAD51L3-XRCC2 complex has a DNA-stimulated ATPase activity and binds preferentially to ssDNA *in vitro*. These properties are similar to those exhibited by the RAD51L3 subunit alone. Indeed, the kinetic parameters for the ATPase activity of the RAD51L3-XRCC2 complex and of RAD51L3 alone are very similar (47), indicating that XRCC2 is unlikely to contribute a powerful ATPase function to the complex. This concurs with the recent finding that cDNAs encoding ATP binding-defective derivatives of XRCC2 are still able to complement defects in the irs1 cell line (XRCC2 deficient), suggesting that at least some functions of XRCC2 are independent of any ATPase activity associated with the protein (42). Nevertheless, it remains possible that XRCC2 modulates the ATPase activity of RAD51L3 under certain circumstances.

Aside from ATPase and DNA binding functions, we have been unable to identify any other biochemical or enzymatic properties of the RAD51L3-XRCC2 complex. These data contrast with the recent findings of Kurumizaka *et al.* (35) who demonstrated that the RAD51L3-XRCC2 complex purified from *E. coli* (using a protocol similar to that described here) could form nucleoprotein filaments and catalyze D-loop formation. Despite rigorous attempts utilizing three independently generated preparations of the RAD51L3-XRCC2 complex (prepared in two independent laboratories) we have been unable to confirm those findings. In our study, we found no evidence that the RAD51L3-XRCC2 complex formed nucleoprotein filaments or could promote D-loop formation. Moreover, the complex did not influence the ability of RAD51 to catalyze formation of D-loops.[2] At this stage, the reason(s) for the discrepancy between our results and those of Kurumizaka *et al.* (35) remains unknown and will require additional investigation. It seems highly unlikely that our preparations of the complex are simply inactive catalytically, because we demonstrated ATPase activity, and binding to both DNA and BLM *in vitro*.

We have shown that the first 212 amino acids of the N-terminal domain of BLM are necessary for mediating an interaction with RAD51L3, although we cannot exclude the possibility that residues that lie outside of this region may also be important for the interaction in the BLM holoenzyme. No interaction with the C-terminal domain of BLM was evident. The extreme N-terminal region of BLM also mediates an interaction with topoisomerase IIIα protein (48). It will be interesting to assess whether there is any competitive or cooperative binding of RAD51L3 and topoisomerase IIIα to BLM. As discussed above, BLM also binds directly to RAD51 (46, 53) and this interaction is mediated via the extreme C-terminal region of BLM (possibly with an additional N-terminal binding site), a pattern of interaction that is conserved in yeast between the BLM homolog, Sgs1p, and the yeast Rad51 protein (46). Whether BLM binds simultaneously to both RAD51 and RAD51L3 will require additional studies.

Individuals with BS are characterized by an enormously high frequency of cancers of most types (1). Although to our knowledge there are no human genetic disorders associated with deficiency in RAD51 paralogs, perhaps because they are encoded by genes essential for cell viability, there are suggestions that polymorphisms in *RAD51* paralog genes may influence cancer risk. Of most relevance to the current study is the recent finding that a polymorphic variant leading to an Arg-188 to His substitution in the XRCC2 protein could be a low penetrance susceptibility factor for breast cancer (54).

Mutations in *BLM* and *RAD51* paralog genes give rise to defects in homologous recombination. However, BLM-defective cell lines exhibit hyper-recombination (2–5), whereas the irs1, irs1SF, and irs3 hamster cell mutants defective in RAD51 paralog function exhibit hypo-recombination and a failure to efficiently carry out homology-directed DNA double strand break (DSB) repair (41, 55, 56). These phenotypic differences might seem at odds with the results represented here showing that BLM interacts functionally with the RAD51L3-XRCC2 complex. However, we would suggest that several lines of evidence indicate that this is not the case. First, mutation of several genes in *S. cerevisiae*, including *MRE11* and *RAD50*, which are required for some aspects of homologous recombination, can confer hyper-recombination (18). Second, there is a conserved interaction between RecQ helicases and more than one component of the homologous recombination machinery, most notably between BLM/Sgs1 and the RAD51 proteins in human and yeast cells (46, 53). Indeed, genetic analyses have shown that mutations in *SGS1* and *RAD51* are epistatic for sensitivity to several DNA damaging agents and replication inhibitors, including methylmethanesulfonate and hydroxurea (46). This strongly suggests that Sgs1p and Rad51p operate in the same biochemical pathway, at least for the cellular response to these agents. Third, BLM co-localizes with RAD51 to sites of presumed ongoing DNA repair in cells treated with DNA damaging agents and replication inhibitors (10, 46, 53). This co-localization occurs following treatment of human cells with agents, such as ionizing radiation, to which BS cells are not obviously hypersensitive. Moreover, not only is BLM recruited to sites of DSB repair (10, 46, 53), but it is also phosphorylated by the ATM kinase following treatment of cells with ionizing radiation (57). Finally, although BS cells are not grossly defective in the repair of DNA DSBs, it is clear that BLM is necessary for ensuring that DSBs are repaired with high fidelity (58, 59). Hence, multiple lines of biochemical, genetic, and cell biological data place BLM alongside the homologous recombination machinery in cells undergoing repair of DNA lesions.

[2] J. P. Braybrooke, J.-L. Li, L. Wu, F. Caple, F. E. Benson, and I. D. Hickson, unpublished data.

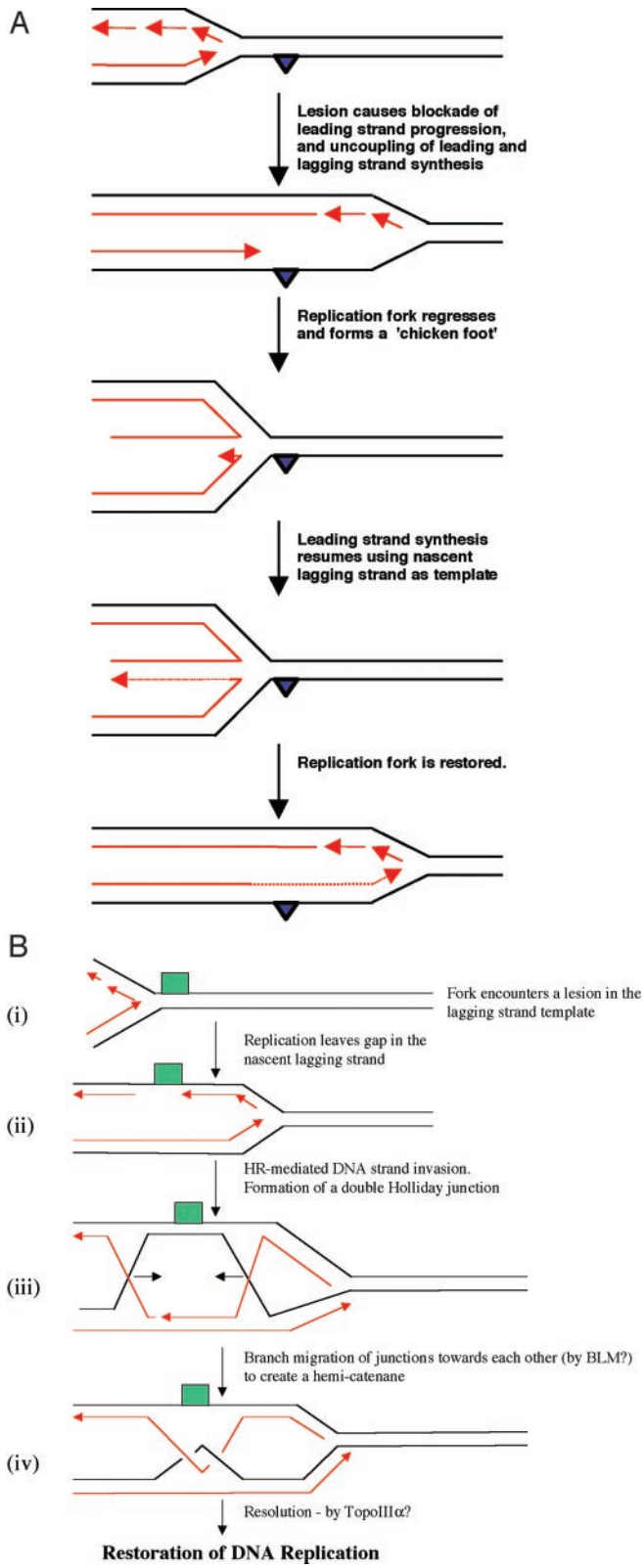

FIG. 6. **Models for the role of BLM in conjunction with the HR machinery in "repair" of damaged replication forks.** *A*, chicken-foot model for the role of RecQ helicases in replication restart. A lesion in the leading strand template (*blue triangle*) blocks leading strand synthesis. However, lagging strand synthesis can continue for a short period. The fork can then regress, allowing the nascent strands to anneal, creating a 4-way junction (chicken-foot). The leading strand can then be extended (*dotted red line*) using the longer lagging strand as a template. The fork can be reset, by a RecQ helicase, by "reverse" branch migration of the 4-way junction. The leading strand has now been extended beyond the site of the lesion, and replication can recommence. *B*, post-replication gap filling model. When a fork encounters a lesion in the lagging strand template (*i*) a gap may be generated in the nascent lagging strand (*ii*). The gap can then be filled by the HR machinery to generate a double Holliday junction (*iii*). The gap is effectively sealed by copying the intact sister-chromatid. The HR intermediate can then be resolved by the combined action of a branch migrating enzyme (*BLM*?) pushing the two junctions toward each other to generate a hemicatenane (*iv*), followed by resolution using a type I topoisomerase, such as topoisomerase III. Note, that the structure in *panel iv* is presented in a highly schematic format with strands of identical sequence being linked, whereas it may be that the links exist between the complementary strands depending upon the degree to which strand invasion is accompanied by intertwining of the complementary strands.

As alluded to above, we do not consider it likely that RecQ helicases participate in bulk DSB repair processes such as following exposure of cells to ionizing radiation. Indeed, evidence suggests that RecQ helicases act primarily during S-phase, probably in a role connected with homologous recombination-mediated repair of damaged replication forks (60, 61). Indeed, it would appear that a major role (and perhaps the primary role) of the homologous recombination machinery is in the maintenance of the structural integrity of replication forks (62). We propose that it is during restoration of productive DNA synthesis following replication fork demise that the BLM, RAD51, and RAD51 paralog proteins associate functionally *in vivo*. Consistent with a role in recovery from replication fork disruption, mutants defective in RecQ helicases, RAD51, and RAD51 paralogs are hypersensitive to killing by agents, such as hydroxyurea, that inhibit DNA replication (46, 63–65). A number of possible roles exist for the RecQ helicases, RAD51, and RAD51 paralog proteins at sites of damaged or stalled replication forks. Given the ability of the RAD51L3-XRCC2 complex to stimulate Holliday junction disruption catalyzed by BLM, and the known function of BLM in suppressing SCEs, we favor a model whereby the proteins act together to process Holliday junctions at sites of stalled forks in such a way as to minimize recombination events associated with crossing over (as would be required to generate SCEs). In Fig. 6, two possible, but not mutually exclusive, roles are presented. In the first, BLM and RAD51 proteins cooperate to "re-set" a replication fork that has regressed at the site of a blocking lesion in the leading strand template (Fig. 6*A*). This regression, which is associated with the formation of a 4-way (Holliday) junction in the context of a so-called "chicken-foot" structure, is caused by annealing of the two nascent DNA strands. In the absence of a RecQ helicase, it is proposed that the regressed fork cannot be re-set, and instead the 4-way junction must be cleaved by an endonuclease or a "resolvase" enzyme to create a DSB at the site of the fork. Re-establishment of a productive fork would then require invasion of the broken end into the homologous sequence, in a process that has the potential to create SCEs.

In a second putative role for BLM and RAD51 paralogs, the complex acts downstream of DNA DSB formation and DNA strand invasion to process Holliday junctions in a manner that excludes crossing over. One possible mechanism by which this could occur is for BLM to act in those cases where double Holliday junctions arise as part of DNA repair processes (such as in the canonical DSB repair model and most models for post-replication filling of ssDNA gaps in the lagging strand). In this model (Fig. 6*B*), BLM processes the double Holliday junction structure by catalyzing branch migration of the two junctions toward each other. This is proposed to convert the double Holliday junction into a so-called hemicatenane structure. Resolution of this structure (decatenation) would complete the repair process without crossover of flanking DNA markers. This latter model has the great attraction of introducing a plausible role for the BLM-associated topoisomerase IIIα pro-

tein, which is known to act as a ssDNA decatenase (66), as would be required for the removal of the hemicatenane structure. Consistent with this model, recent data suggest that the RAD51 paralogs may also act late in homologous recombination reactions, possibly at a stage during the processing of Holliday junctions (67). Moreover, at least one RAD51 paralog, RAD51B, appears to bind selectively to Holliday junctions compared with double strand DNA or ssDNA (68). The functional interaction of BLM and RAD51L3-XRCC2 would be consistent with a combined role for these proteins in the branch migration of Holliday junctions to effect their "resolution" in ways that exclude SCE formation.

In summary, we have shown that the BLM helicase interacts physically and functionally with the RAD51L3-XRCC2 heteromeric complex. This strengthens existing data linking BLM to processes involved in the homologous recombinational repair of DNA damages arising during S-phase. Given the key role that BLM plays as a tumor suppressor in humans, it is important to extend our knowledge of the key protein interactions mediated by BLM and to delineate in greater detail the biological roles of these multienzyme complexes.

Acknowledgments—We thank members of the Benson and Hickson laboratories for valuable discussions, Drs. S. C. West, J. Y. Masson, and M. McIlwraith for RAD51 protein and helpful advice, and J. Pepper for preparation of the manuscript.

REFERENCES

1. German, J. (1995) *Dermatol. Clin.* **13,** 7–18
2. van Brabant, A. J., Stan, R., and Ellis, N. A. (2000) *Annu. Rev. Genomics Hum. Genet.* **1,** 409–459
3. Karow, J. K., Wu, L., and Hickson, I. D. (2000) *Curr. Opin. Genet. Dev.* **10,** 32–38
4. Hickson, I. D. (2003) *Nat. Rev. Cancer* **3,** 169–178
5. Chaganti, R. S., Schonberg, S., and German, J. (1974) *Proc. Natl. Acad. Sci. U. S. A.* **71,** 4508–4512
6. Ellis, N. A., Groden, J., Ye, T. Z., Straughen, J., Lennon, D. J., Ciocci, S., Proytcheva, M., and German, J. (1995) *Cell* **83,** 655–666
7. Yu, C., Oshima, J., Fu, Y., Wijsman, E. M., Hisama, F., Alisch, R., Matthews, S., Najura, J., Miki, T., Ouais, S., Martin, G. M., Mulligan, J., and Schellenberg, G. D. (1996) *Science* **272,** 258–262
8. Kitao, S., Shimamoto, A., Goto, M., Miller, R. W., Smithson, W. A., Lindor, N. M., and Furuichi, Y. (1999) *Nat. Genet.* **22,** 82–84
9. Mohaghegh, P., Karow, J. K., Brosh, R. M., Jr., Bohr, V. A., Jr., and Hickson, I. D. (2001) *Nucleic Acids Res.* **29,** 2843–2849
10. Wu, X., and Maizels, N. (2001) *Nucleic Acids Res.* **29,** 1765–1771
11. Sun, H., Karow, J. K., Hickson, I. D., and Maizels, N. (1998) *J. Biol. Chem.* **273,** 27587–27592
12. Sun, H., Bennett, R. J., and Maizels, N. (1999) *Nucleic Acids Res.* **27,** 1978–1984
13. Fry, M., and Loeb, L. A. (1999) *J. Biol. Chem.* **274,** 12797–12802
14. van Brabant, A. J., Ye, T., Sanz, M., German, I. J., Ellis, N. A., and Holloman, W. K. (2000) *Biochemistry* **39,** 14617–14625
15. Karow, J. K., Constantinou, A., Li, J. L., West, S. C., and Hickson, I. D. (2000) *Proc. Natl. Acad. Sci. U. S. A.* **97,** 6504–6508
16. Harmon, F. G., and Kowalczykowski, S. C. (2001) *J. Biol. Chem.* **276,** 232–243
17. Constantinou, A., Tarsounas, M., Karow, J. K., Brosh, R. M., Bohr, V. A., Hickson, I. D., and West, S. C. (2000) *EMBO Rep.* **1,** 80–84
18. Paques, F., and Haber, J. E. (1999) *Microbiol. Mol. Biol. Rev.* **63,** 349–404
19. West, S. C. (2003) *Nat. Rev. Mol. Cell. Biol.* **4,** 435–445
20. Johnson, R. D., and Symington, L. S. (1995) *Mol. Cell. Biol.* **15,** 4843–4850
21. Sung, P. (1997) *Genes Dev.* **11,** 1111–1121
22. Cartwright, R., Dunn, A. M., Simpson, P. J., Tambini, C. E., and Thacker, J. (1998) *Nucleic Acids Res.* **26,** 1653–1659
23. Liu, N., Lamerdin, J. E., Tebbs, R. S., Schild, D., Tucker, J. D., Shen, M. R., Brookman, K. W., Siciliano, M. J., Walter, C. A., Fan, W., Narayana, L. S., Zhou, Z. Q., Adamson, A. W., Sorensen, K. J., Chen, D. J., Jones, N. J., and Thompson, L. H. (1998) *Mol. Cell* **1,** 783–793
24. Tebbs, R. S., Zhao, Y., Tucker, J. D., Scheerer, J. B., Siciliano, M. J., Hwang, M., Liu, N., Legerski, R. J., and Thompson, L. H. (1995) *Proc. Natl. Acad. Sci. U. S. A.* **92,** 6354–6358
25. Albala, J. S., Thelen, M. P., Prange, C., Fan, W., Christensen, M., Thompson, L. H., and Lennon, G. G. (1997) *Genomics* **46,** 476–479
26. Rice, M. C., Smith, S. T., Bullrich, F., Havre, P., and Kmiec, E. B. (1997) *Proc. Natl. Acad. Sci. U. S. A.* **94,** 7417–7422
27. Cartwright, R., Tambini, C. E., Simpson, P. J., and Thacker, J. (1998) *Nucleic Acids Res.* **26,** 3084–3089
28. Dosanjh, M. K., Collins, D. W., Fan, W., Lennon, G. G., Albala, J. S., Shen, Z., and Schild, D. (1998) *Nucleic Acids Res.* **26,** 1179–1184
29. Kawabata, M., and Saeki, K. (1999) *Biochem. Biophys. Res. Commun.* **257,** 156–162
30. Pittman, D. L., Weinberg, L. R., and Schimenti, J. C. (1998) *Genomics* **49,** 103–111
31. Thacker, J., and Zdzienicka, M. Z. (2003) *DNA Repair* **2,** 655–672
32. Jones, N. J., Cox, R., and Thacker, J. (1987) *Mutat. Res.* **183,** 279–286
33. Fuller, L. F., and Painter, R. B. (1988) *Mutat. Res.* **193,** 109–121
34. Griffin, C. S., Simpson, P. J., Wilson, C. R., and Thacker, J. (2000) *Nat. Cell Biol.* **2,** 757–761
35. Kurumizaka, H., Ikawa, S., Nakada, M., Enomoto, R., Kagawa, W., Kinebuchi, T., Yamazoe, M., Yokoyama, S., and Shibata, T. (2002) *J. Biol. Chem.* **277,** 14315–14320
36. Masson, J. Y., Tarsounas, M. C., Stasiak, A. Z., Stasiak, A., Shah, R., McIlwraith, M. J., Benson, F. E., and West, S. C. (2001) *Genes Dev.* **15,** 3296–3307
37. Masson, J. Y., Stasiak, A. Z., Stasiak, A., Benson, F. E., and West, S. C. (2001) *Proc. Natl. Acad. Sci. U. S. A.* **98,** 8440–8446
38. Sigurdsson, S., Van Komen, S., Bussen, W., Schild, D., Albala, J. S., and Sung, P. (2001) *Genes Dev.* **15,** 3308–3318
39. Liu, N., Schild, D., Thelen, M. P., and Thompson, L. H. (2002) *Nucleic Acids Res.* **30,** 1009–1015
40. Bishop, D. K., Ear, U., Bhattacharyya, A., Calderone, C., Beckett, M., Weichselbaum, R. R., and Shinohara, A. (1998) *J. Biol. Chem.* **273,** 21482–21488
41. French, C. A., Masson, J. Y., Griffin, C. S., O'Regan, P., West, S. C., and Thacker, J. (2002) *J. Biol. Chem.* **277,** 19322–19330
42. O'Regan, P., Wilson, C., Townsend, S., and Thacker, J. (2001) *J. Biol. Chem.* **276,** 22148–22153
43. Brosh, R. M., Jr., Orren, D. K., Nehlin, J. O., Ravn, P. H., Kenny, M. K., Machwe, A., and Bohr, V. A. (1999) *J. Biol. Chem.* **274,** 18341–18350
44. Brosh, R. M., Jr., Li, J. L., Kenny, M. K., Karow, J. K., Cooper, M. P., Kureekattil, R. P., Hickson, I. D., and Bohr, V. A. (2000) *J. Biol. Chem.* **275,** 23500–23508
45. Cui, S., Klima, R., Ochem, A., Arosio, D., Falaschi, A., and Vindigni, A. (2003) *J. Biol. Chem.* **278,** 1424–1432
46. Wu, L., Davies, S. L., Levitt, N. C., and Hickson, I. D. (2001) *J. Biol. Chem.* **276,** 19375–19381
47. Braybrooke, J. P., Spink, K. G., Thacker, J., and Hickson, I. D. (2000) *J. Biol. Chem.* **275,** 29100–29106
48. Wu, L., Davies, S. L., North, P. S., Goulaouic, H., Riou, J. F., Turley, H., Gatter, K. C., and Hickson, I. D. (2000) *J. Biol. Chem.* **275,** 9636–9644
49. Brent, R., and Ptashne, M. (1985) *Cell* **43,** 729–736
50. Gietz, D., St. Jean, A., Woods, R. A., and Schiestl, R. H. (1992) *Nucleic Acids Res.* **20,** 1425
51. Zervos, A. S., Gyuris, J., and Brent, R. (1993) *Cell* **72,** 223–232
52. Wu, L., and Hickson, I. D. (2002) *Nucleic Acids Res.* **30,** 4823–4829
53. Bischof, O., Kim, S. H., Irving, J., Beresten, S., Ellis, N. A., and Campisi, J. (2001) *J. Cell Biol.* **153,** 367–380
54. Rafii, S., O'Regan, P., Xinarianos, G., Azmy, I., Stephenson, T., Reed, M., Meuth, M., Thacker, J., and Cox, A. (2002) *Hum. Mol. Genet.* **11,** 1433–1438
55. Johnson, R. D., Liu, N., and Jasin, M. (1999) *Nature* **401,** 397–399
56. Pierce, A. J., Johnson, R. D., Thompson, L. H., and Jasin, M. (1999) *Genes Dev.* **13,** 2633–2638
57. Beamish, H., Kedar, P., Kaneko, H., Chen, P., Fukao, T., Peng, C., Beresten, S., Gueven, N., Purdie, D., Lees-Miller, S., Ellis, N., Kondo, N., and Lavin, M. F. (2002) *J. Biol. Chem.* **277,** 30515–30523
58. Langland, G., Elliott, J., Li, Y., Creaney, J., Dixon, K., and Groden, J. (2002) *Cancer Res.* **62,** 2766–2770
59. Gaymes, T. J., North, P. S., Brady, N., Hickson, I. D., Mufti, G. J., and Rassool, F. V. (2002) *Oncogene* **21,** 2525–2533
60. Chakraverty, R. K., and Hickson, I. D. (1999) *BioEssays* **21,** 286–294
61. Oakley, T., and Hickson, I. D. (2002) *DNA Repair* **1,** 175–207
62. McGlynn, P., and Lloyd, R. G. (2002) *Nat. Rev. Mol. Cell. Biol.* **3,** 859–870
63. Lundin, C., Erixon, K., Arnaudeau, C., Schultz, N., Jenssen, D., Meuth, M., and Helleday, T. (2002) *Mol. Cell. Biol.* **22,** 5869–5878
64. Stewart, E., Chapman, C. R., Al-Khodairy, F., Carr, A. M., and Enoch, T. (1997) *EMBO J.* **16,** 2682–2692
65. Frei, C., and Gasser, S. M. (2000) *Genes Dev.* **14,** 81–96
66. Champoux, J. J. (2001) *Annu. Rev. Biochem.* **70,** 369–413
67. Brenneman, M. A., Wagener, B. M., Miller, C. A., Allen, C., and Nickoloff, J. A. (2002) *Mol. Cell* **10,** 387–395
68. Yokoyama, H., Kurumizaka, H., Ikawa, S., Yokoyama, S., and Shibata, T. (2003) *J. Biol. Chem.* **278,** 2767–2772

Functional Interaction between the Bloom's Syndrome Helicase and the RAD51 Paralog, RAD51L3 (RAD51D)

Jeremy P. Braybrooke, Ji-Liang Li, Leonard Wu, Fiona Caple, Fiona E. Benson and Ian D. Hickson

J. Biol. Chem. 2003, 278:48357-48366.
doi: 10.1074/jbc.M308838200 originally published online September 15, 2003
